

# Solid-state $^{17}\text{O}$ NMR Study of Small Biological Compounds

Kazuhiko Yamada<sup>a</sup>, Tadashi Shimizu<sup>b</sup>, Mitsuru Yoshida<sup>c</sup>, Miwako Asanuma<sup>a</sup>, Masataka Tansho<sup>b</sup>, Takahiro Nemoto<sup>d</sup>, Toshio Yamazaki<sup>a</sup>, and Hiroshi Hirota<sup>a</sup>

<sup>a</sup> RIKEN Genomic Sciences Center, 1-7-22 Suehiro, Tsurumi, Yokohama, 230-0045 Japan

<sup>b</sup> Tsukuba Magnet Laboratory, National Institute for Materials Science, 3-13 Sakura, Tsukuba, 305-0003 Japan

<sup>c</sup> Analytical Science Division, National Food Research Institute, 2-1-12 Kannondai, Tsukuba, 305-8642 Japan

<sup>d</sup> Analytical R&D team NM/ER Group, Analytical Instrument Division, JEOL Ltd, 3-1-2 Musashino Akishima, Tokyo, 189-8558 Japan

Reprint requests to Dr. K. Yamada. Fax: +81-45-503-9228. E-mail: kyamada@gsc.riken.jp

*Z. Naturforsch.* **2007**, *62b*, 1422 – 1432; received April 6, 2007

We present a systematic experimental and theoretical investigation of the oxygen chemical shielding and electric-field-gradient tensors in polycrystalline amino acids and a peptide. Analysis of the  $^{17}\text{O}$  magic-angle-spinning (MAS), multiple-quantum MAS, and stationary nuclear magnetic resonance (NMR) spectra yield the magnitudes and the relative orientations between the two NMR tensors. The obtained  $^{17}\text{O}$  NMR parameters are sensitive to the hydrogen bond environments. We also demonstrate that solid-state  $^{17}\text{O}$  NMR is potentially useful for studying the secondary structures of peptides and proteins.

**Key words:** Solid-state  $^{17}\text{O}$  NMR, Electric-field-gradient Tensor, Chemical Shielding Tensor, Amino Acid, Peptide

## Introduction

Oxygen-containing functional groups play crucial roles in numerous biological functions. Nevertheless, the research field of oxygen solid-state nuclear magnetic resonance (NMR) in organic and biological molecules was much less developed compared to other common nuclei such as hydrogen, carbon and nitrogen. The oxygen-17 isotope,  $^{17}\text{O}$ , is the only NMR accessible nucleus (natural abundance = 0.037%,  $\gamma = -3.6279 \times 10^7 \text{ rad T}^{-1} \text{ s}^{-1}$ ,  $Q(^{17}\text{O}) = -2.6 \text{ fm}^2$ ) among the oxygen stable isotopes, but its unfavorable properties have made it difficult to routinely carry out solid-state  $^{17}\text{O}$  NMR experiments. One of the major problems associated with solid-state  $^{17}\text{O}$  NMR studies of organic/biological molecules is severe line broadening due to relatively large quadrupolar interactions. Due to recent developments such as the introduction of high-field magnets and invention of efficient NMR techniques for half-integer quadrupolar nuclei [1, 2], however, solid-state  $^{17}\text{O}$  NMR has become accessible in chemistry and biochemistry. In particular, there are tremendous advantages of performing  $^{17}\text{O}$  NMR experiments at higher magnetic fields.

The aim of our research is to apply solid-state  $^{17}\text{O}$  NMR to protein research in the future. The obtained NMR parameters from solid-state  $^{17}\text{O}$  NMR are the chemical shielding (CS) and electric-field-gradient (EFG) tensors, which are expected to be sensitive to the local electronic structures. At the present time, there are several papers reporting  $^{17}\text{O}$  NMR determination of biological compounds such as amino acids and peptides [3–7]. Since the natural abundance is extremely low,  $^{17}\text{O}$  isotope enrichment is generally required for biological molecules. For typical preparations of  $^{17}\text{O}$ -enriched amino acids, the amino acids are synthesized by acid-catalyzed exchange with  $^{17}\text{O}$ -enriched water at high temperature [8].  $^{17}\text{O}$ -enriched peptides can be synthesized on the basis of a solid phase peptide synthesis (SPPS) protocol by using the  $^{17}\text{O}$  labeled amino acids which are *N*-protected by introduction of a 9-fluorenylmethoxycarbonyl (Fmoc) or *t*-butoxycarbonyl (Boc) group [7]. Since the acid-catalyzed exchange reactions are only allowed to proceed under severe experimental conditions, *e. g.*, an amino acid solution is saturated with HCl gas at 100 °C, some amino acids may be decomposed. Moreover, the rate of racemization may in-

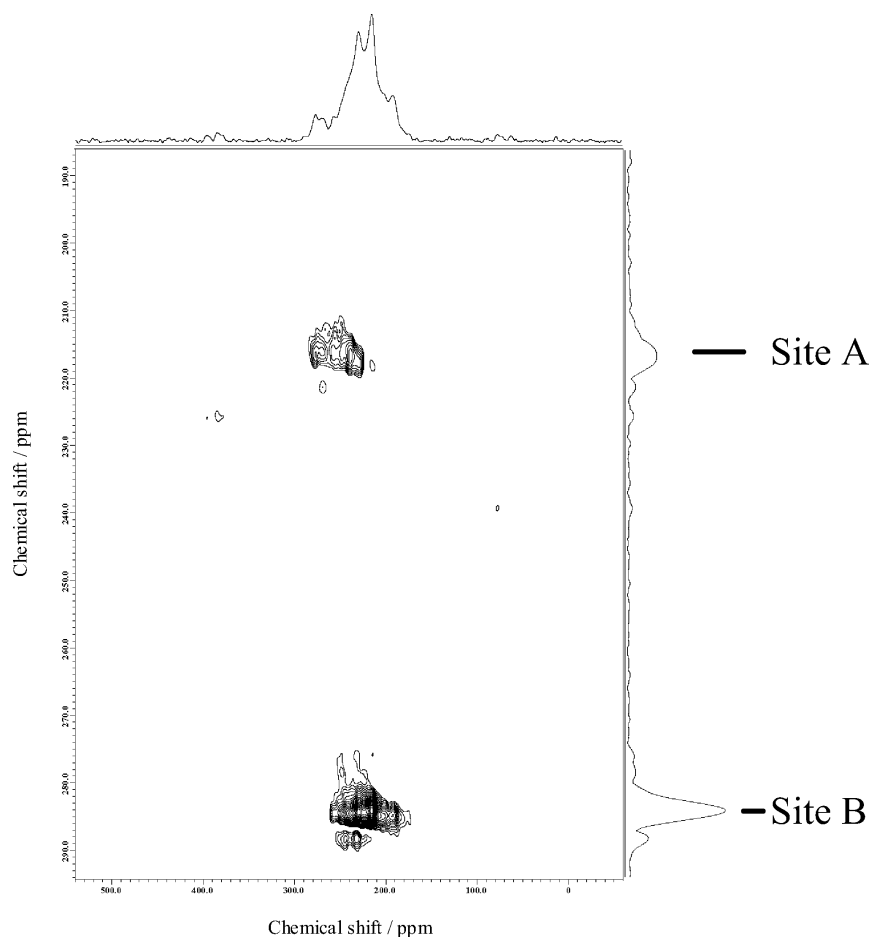


Fig. 1. Contour plot of the  $^{17}\text{O}$   $z$ -filter 3QMCMAS spectrum of  $[^{17}\text{O}]$ -L-glutamine observed at 16.4 T. The lengths of the first and second hard pulses were 4.5  $\mu\text{s}$  and 1.3  $\mu\text{s}$ , respectively. The soft pulse length was 20  $\mu\text{s}$ . The recycle delay was 5 s. 128 data points were acquired in the  $t_1$  dimensions with 576 transients per point.

crease. Recently, an efficient synthetic route for  $^{17}\text{O}$  enrichment in Fmoc/Boc protected amino acids under moderate experimental conditions has been reported [9]. The method has the advantage that almost all kinds of amino acids can be  $^{17}\text{O}$ -enriched. Another advantage is that  $^{17}\text{O}$ -enriched Fmoc-protected amino acids can be directly used for the SPPS protocol. Overall, it enables to conveniently carry out solid-state  $^{17}\text{O}$  NMR experiments of any kind of amino acids and peptides, which are a good starting point for future application to proteins. In this paper, we report solid-state  $^{17}\text{O}$  NMR determination of CS and EFG tensors for a series of  $^{17}\text{O}$ -enriched small biological compounds: L-glutamine, L-asparagine, L-cystine, L-histidine, and L-tryptophanyl-glycyl-glycine dihydrate. This work is part of a systematic investigation of amino acids, peptides, and proteins by solid-state  $^{17}\text{O}$  NMR spectroscopy performed at RIKEN Genomic Sciences Center.

## Results and Discussion

### Amino acids

For solid-state  $^{17}\text{O}$  NMR spectroscopy of organic and biological compounds, the obtained NMR parameters are mainly CS and EFG tensors ( $\delta_{11}$ ,  $\delta_{22}$ ,  $\delta_{33}$ ,  $C_Q$ , and  $\eta_Q$ ). In general, the two NMR tensors have different orientations with respect to the molecular frame, and three Euler angles ( $\alpha$ ,  $\beta$ ,  $\gamma$ ) are used to express the relative orientations between the tensors. Thus, from spectral simulations of  $^{17}\text{O}$  NMR line shapes, a total of eight independent NMR parameters can be obtained for each oxygen site. The detailed procedure for the spectral analysis of  $^{17}\text{O}$  NMR spectra was previously reported [10]. In the cases of polycrystalline amino acids which generally take zwitterionic forms, a total of sixteen independent NMR parameters are obtained for the two carboxylate oxygen sites.

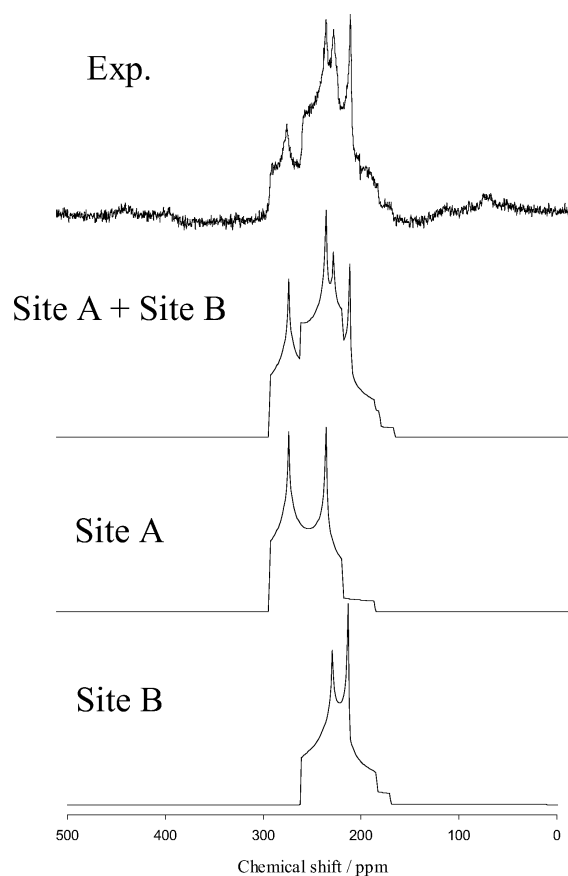


Fig. 2. Experimental and calculated 1D  $^{17}\text{O}$  MAS spectra of  $^{17}\text{O}$ -L-glutamine measured at 16.4 T.

Fig. 1 shows the contour plot of the  $^{17}\text{O}$  triple-quantum MQMAS spectra of  $^{17}\text{O}$ -L-glutamine obtained with rotor synchronization for the  $t_1$  increments in which the sample spinning frequency was set at  $14.61 \pm 0.05$  kHz. Both the F1 and F2 projections of the 2D MQMAS spectra are also given on the side and at the top, respectively. Two well-resolved peaks, marked as site A and site B, can be seen. Analysis of each cross-section spectrum along the F2 dimension provides information on  $\delta_{\text{iso}}$ ,  $C_Q$ , and  $\eta_Q$  for each site. However, such cross-section spectra are very often distorted by multiple-quantum effects. Moreover, quantitative information of MQMAS spectra is not reliable. Therefore, the NMR parameters estimated from analysis of MQMAS spectra were only used for initial values in the simulations of 1D MAS spectra. Final  $^{17}\text{O}$  NMR parameters were extracted by analysis of the 1D MAS spectra observed at 16.4 T, as shown in Fig. 2. The analysis of the combined 2D MQMAS

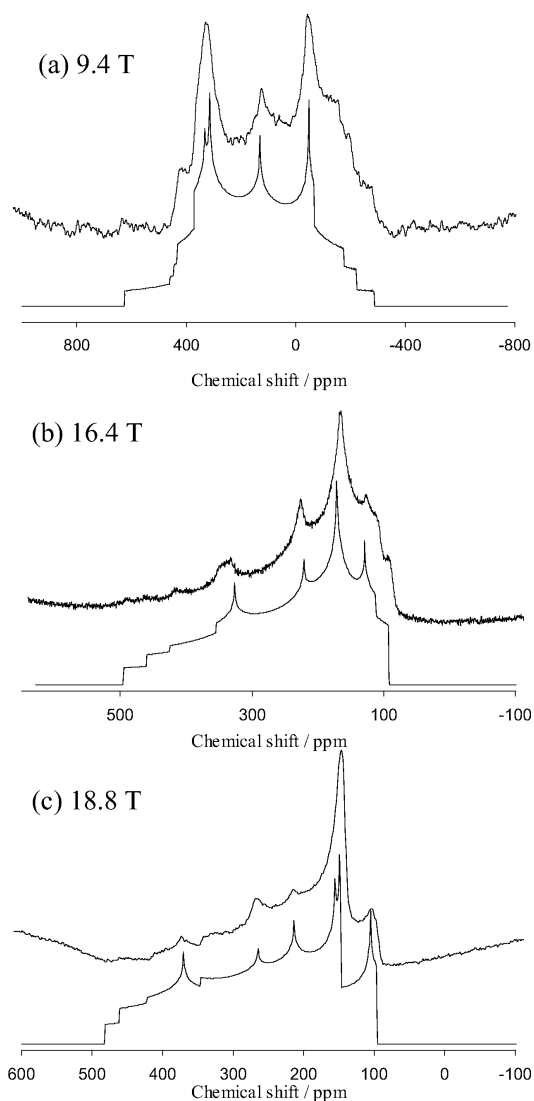


Fig. 3. Experimental and calculated  $^{17}\text{O}$  stationary spectra of  $^{17}\text{O}$ -L-glutamine observed at (a) 9.4, (b) 16.4, and (c) 18.8 T.

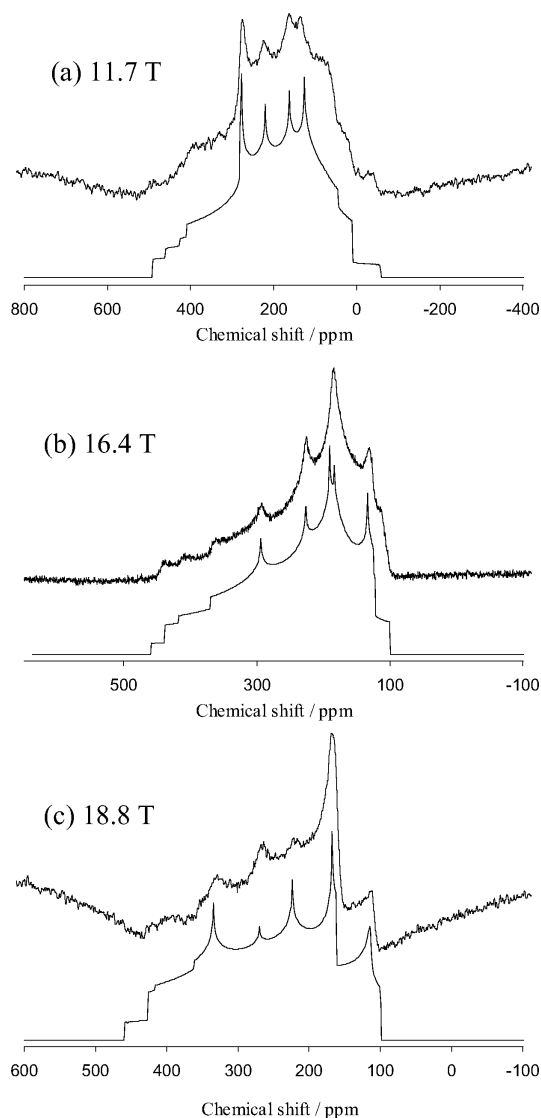
and 1D MAS spectra yielded the following parameters for L-glutamine: site A,  $\delta_{\text{iso}} = 301 \pm 1$  ppm,  $C_Q = 8.10 \pm 0.02$  MHz,  $\eta_Q = 0.30 \pm 0.02$ ; site B,  $\delta_{\text{iso}} = 265 \pm 1$  ppm,  $C_Q = 7.25 \pm 0.02$  MHz,  $\eta_Q = 0.65 \pm 0.02$ .

In order to obtain  $^{17}\text{O}$  CS tensor components, analysis of stationary  $^{17}\text{O}$  NMR line shapes is required. In most cases, stationary  $^{17}\text{O}$  NMR spectra of organic/biological molecules exhibit very complicated line shapes. As we suggested in recent studies [11, 12], however,  $^{17}\text{O}$  NMR tensors can be unambiguously derived from the simultaneous analysis of powder

	$\delta_{11}$	$\delta_{22}$	$\delta_{33}$	$\delta_{\text{iso}}$	$C_Q$	$\eta_Q$	$\alpha$	$\beta$	$\gamma$
L-glutamine									
site A	516(4)	357(4)	30(4)	301(1)	8.10(5)	0.30(2)	0(4)	90(4)	140(4)
site B	434(4)	286(4)	75(4)	265(1)	7.25(5)	0.65(2)	0(4)	90(4)	156(4)
L-asparagine									
site A	482(4)	348(4)	40(4)	290(1)	7.70(5)	0.35(2)	0(4)	88(4)	152(4)
site B	430(4)	300(4)	95(4)	275(1)	7.30(5)	0.60(2)	0(4)	90(4)	154(4)
L-cystine									
site A	482(4)	346(4)	39(4)	289(1)	7.60(5)	0.46(2)	0(4)	95(4)	147(4)
site B	465(4)	310(4)	59(4)	278(1)	7.00(5)	0.62(2)	1(4)	90(4)	142(4)
L-histidine									
site A	460(4)	328(4)	46(4)	278(1)	7.35(5)	0.40(2)	0(4)	92(4)	149(4)
site B	430(4)	318(4)	77(4)	275(1)	7.50(5)	0.55(2)	0(4)	90(4)	150(4)
WGG	535(9)	400(9)	-44(9)	297(4)	8.4(1)	0.24(4)	0(6)	90(6)	108(6)

Table 1. Experimental  $^{17}\text{O}$  CS, EFG tensors and Euler angles for L-glutamine, L-asparagine, L-cystine, L-histidine, and L-tryptophanyl-glycyl-glycine (WGG).<sup>a</sup>

<sup>a</sup> Errors in the last digits are given in parentheses; chemical shifts in ppm,  $C_Q$  in MHz, angles in degrees.



← Fig. 4. Experimental and calculated  $^{17}\text{O}$  stationary spectra of  $^{17}\text{O}$ -L-asparagine observed at (a) 11.7, (b) 16.4, and (c) 18.8 T.

line shapes recorded at multiple magnetic fields. The experimental and best-fitted calculated  $^{17}\text{O}$  stationary NMR spectra of  $^{17}\text{O}$ -L-glutamine observed at (a) 9.4, (b) 16.4, and (c) 18.8 T are shown in Fig. 3. The obtained experimental  $^{17}\text{O}$  NMR parameters for L-glutamine are summarized in Table 1.

Likewise, experimental and best-fitted calculated  $^{17}\text{O}$  stationary NMR spectra for L-asparagine, L-cystine, and L-histidine observed at multiple magnetic fields are shown in Figs. 4–6, respectively. The corresponding magnetic fields used in the experiments are also shown in the figures. The experimental  $^{17}\text{O}$  NMR parameters are summarized in Table 1.

The present data of L-glutamine, for example, indicate that two carboxylate oxygen atoms experience quite different chemical environments. It can be expected that such differences are mainly attributed to the different hydrogen bond environments. Fig. 7(a) displays the schematic representation of the hydrogen bond geometry for L-glutamine with C–O bond and hydrogen bond lengths [13]. As seen, O1 is involved in one hydrogen bond, while O2 entertains two hydrogen bonds. Moreover, the C–O2 bond length (1.260 Å) is longer than the C–O1 bond length (1.238 Å). Hence, O2 is clearly involved in a stronger hydrogen bonding environment. Previously, the relationship between  $^{17}\text{O}$  NMR parameters and hydrogen bond strengths was discussed both theoretically and experimentally [6, 10, 12] and it was established that the values of  $^{17}\text{O}$   $\delta_{\text{iso}}$  and  $C_Q$  tend to decrease with increase in hydrogen bond strength. Therefore, it can be concluded that site A is assigned to be O1. To con-

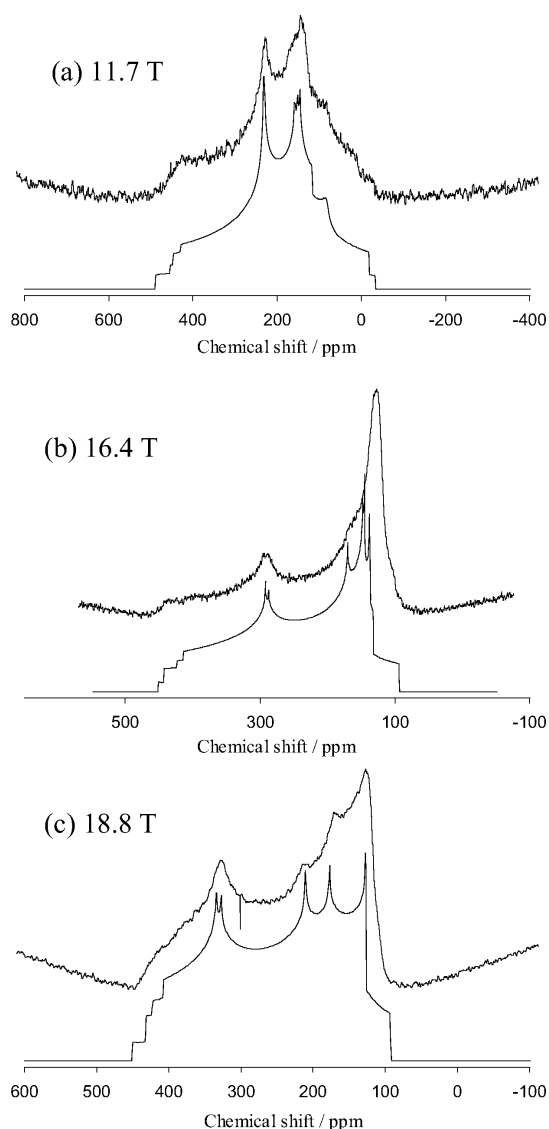


Fig. 5. Experimental and calculated  $^{17}\text{O}$  stationary spectra of  $^{17}\text{O}$ -L-cystine observed at (a) 11.7, (b) 16.4, and (c) 18.8 T.

firm the present assignment, we carried out quantum chemical calculations for the  $^{17}\text{O}$  NMR parameters on the B3LYP/D95\*\* level of theory. The results for L-glutamine are summarized in Table 2. It is seen that the values of  $\delta_{\text{iso}}$  and  $C_Q$  for O1 are larger than those for O2. Apparently, the values of other NMR parameters for both oxygen sites reproduce the corresponding experimental data, which supports the present spectral assignment.

The schematic representation of the hydrogen bonding geometry for L-cystine [14] and the calculated re-

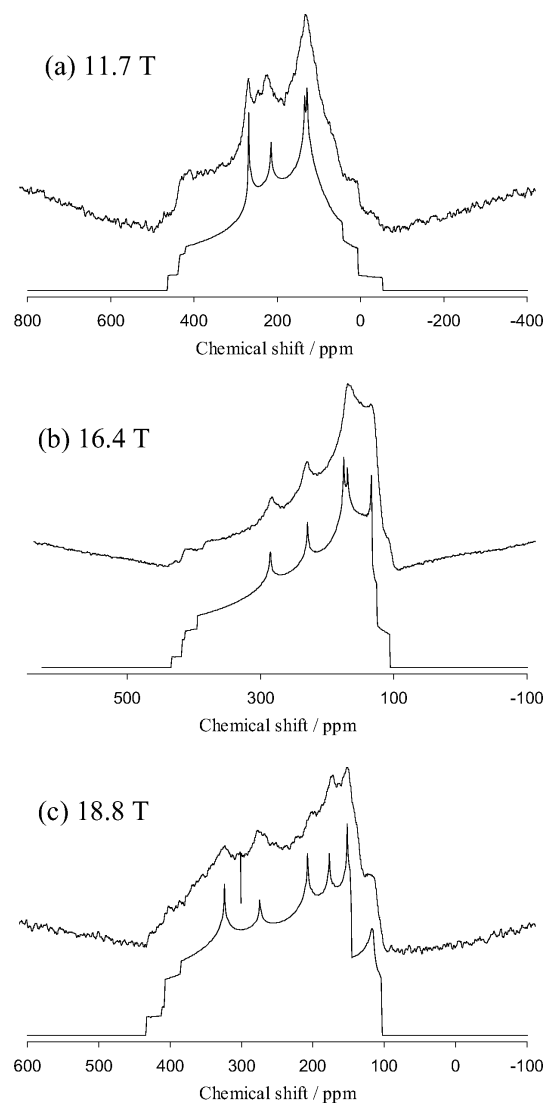


Fig. 6. Experimental and calculated  $^{17}\text{O}$  stationary spectra of  $^{17}\text{O}$ -L-histidine observed at (a) 11.7, (b) 16.4, and (c) 18.8 T.

sults for the  $^{17}\text{O}$  NMR parameters are given in Fig. 7(b) and Table 2, respectively. In a manner similar to the case of L-glutamine, it can be concluded that site A is assigned to be O1 for L-cystine.

Spectral assignment is not readily achieved on the basis of the crystal structure of L-histidine [15]. As seen in Fig. 7(c), each oxygen atom is involved in two hydrogen bonds so that it is difficult to judge the hydrogen bond strengths by the above criteria. The calculated results for  $^{17}\text{O}$  NMR parameters of L-histidine are summarized in Table 2. It can be seen that the val-

	$\delta_{11}$	$\delta_{22}$	$\delta_{33}$	$\delta_{\text{iso}}$	$C_Q$	$\eta_Q$	$\alpha$	$\beta$	$\gamma$
L-glutamine									
O1(site A)	538.1	381.7	37.0	318.9	8.72	0.35	-2.0	90.1	138.1
O2(site B)	455.2	311.2	83.0	283.2	7.77	0.69	-0.4	88.9	153.7
L-cystine									
O1(site A)	548.2	403.3	56.2	335.9	8.34	0.39	0.5	92.2	139.5
O2(site B)	436.8	285.8	59.0	260.6	7.64	0.78	0.0	92.2	143.2
L-histidine									
O1(site A)	485.2	343.5	59.9	296.2	8.28	0.49	-2.7	89.7	147.2
O2(site B)	471.8	340.6	76.2	296.2	8.13	0.55	-0.3	91.9	148.4
WGG	525.6	419.0	-49.3	298.4	8.64	0.50	1.1	91.9	103.6

Table 2. Calculated  $^{17}\text{O}$  CS, EFG tensors and Euler angles for L-glutamine, L-cystine, L-histidine, and L-tryptophanyl-glycyl-glycine (WGG).<sup>a</sup>

<sup>a</sup> Chemical shifts in ppm,  $C_Q$  in MHz, angles in degrees.

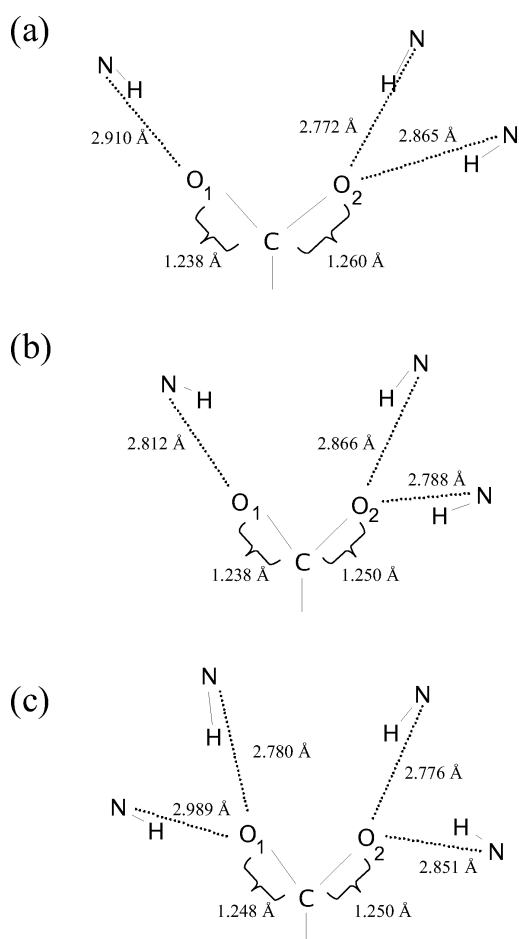


Fig. 7. The hydrogen bonding geometries of (a) L-glutamine, (b) L-cystine, and (c) L-histidine.

ues of  $\delta_{\text{iso}}$  for O1 and O2 are essentially the same (296.2 ppm), while those of the  $\delta_{11}$  and  $\delta_{22}$  components and  $C_Q$  for O1 are slightly larger than those for O2. It should be noted that, at the present time, quantum chemical calculations can reasonably reproduce the experimental data, but it is nearly impossible

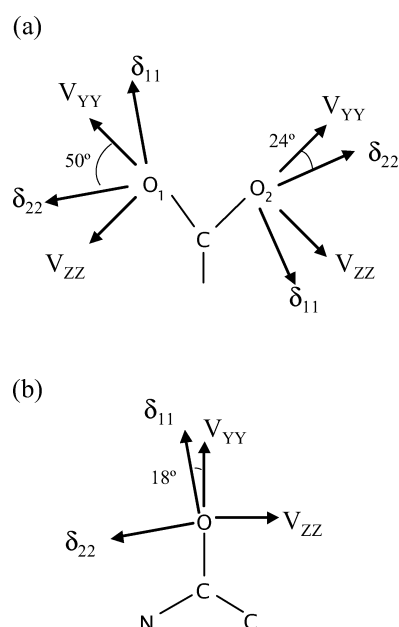


Fig. 8. Orientations of  $^{17}\text{O}$  EFG and CS tensors in the molecular frames of (a)  $^{17}\text{O}$ -L-glutamine and (b)  $^{17}\text{O}$ -L-tryptophanyl-glycyl-glycine dihydrate.

to predict them without errors. Hence, for very similar chemical environments, it would be dangerous to assign oxygen sites only on the basis of the calculated results. The spectral assignment for L-histidine shall be discussed later.

Unfortunately, the crystal structure of L-asparagine has not yet been reported so that the spectral assignment is not possible at this time. As compared to the  $^{17}\text{O}$  NMR data of other amino acids, however, it is expected that the L-asparagine molecule takes a zwitterionic form and the two oxygen atoms experience quite different chemical environments, *i. e.*, site B is involved in stronger hydrogen bonds than site A.

It is important to note that the NMR line shapes shown in Figs. 3–6 are only dependent on the rel-

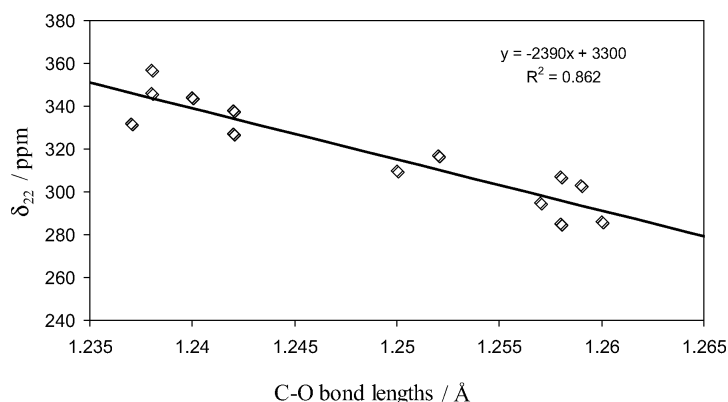


Fig. 9. C–O bond length dependence of the values for  $\delta_{22}$  components in a series of amino acids.

ative orientation between the  $^{17}\text{O}$  CS and EFG tensors. To establish the absolute tensor orientation in the molecular frame, it was assumed that the orientations of the  $^{17}\text{O}$  EFG tensors obtained from high-level quantum chemical calculations were correct. With the combined results of the absolute orientations for EFG tensors and the Euler angles determined experimentally, it was feasible to determine the absolute orientations of  $^{17}\text{O}$  CS tensors with respect to the molecular frame [10]. The  $^{17}\text{O}$  NMR tensor orientations for L-glutamine are shown in Fig. 8(a). The orientations of the  $^{17}\text{O}$  EFG tensors are essentially the same at both oxygen sites. For O1 and O2, the smallest EFG tensor components,  $V_{XX}$ , are approximately perpendicular to the molecular plane (O1–C–O2), and the  $V_{YY}$  components are roughly parallel to the C–O bond directions. On the other hand, the CS tensors for O1 and O2 have slightly different CS tensor orientations. For both oxygen sites, the most shielding components,  $\delta_{33}$ , are approximately perpendicular to the molecular plane. The  $\delta_{22}$  component for O1 lies in the O1–C–O2 plane approximately  $50^\circ$  off the C–O bond direction, while for O2 the value is approximately  $24^\circ$ . These observations are in reasonable agreement with previous determinations for other amino acids [11, 12]. The results suggest that, in addition to the magnitudes, CS tensor orientations are also sensitive to chemical environments, *e. g.*, hydrogen bond strengths.

It was demonstrated [4, 16] that  $^{17}\text{O}$  NMR parameters such as  $\delta_{\text{iso}}$  and  $C_Q$  are related to the corresponding C–O bond lengths for some biological molecules. Recently, instead of isotropic values, we have reported  $^{17}\text{O}$  NMR tensors for a series of amino acids [11, 12, 17]. Obviously, it is more advantageous to analyze NMR tensor components than isotropic values for investigating physicochemical properties in a

variety of biological compounds. It was found that there was a significant correlation between the magnitudes of  $\delta_{22}$  components and C–O bond lengths. Such a correlation for amino acids is plotted in Fig. 9. As seen, the values of  $\delta_{22}$  components tend to linearly decrease with an increase in C–O bond lengths, *i.e.*, hydrogen bond strengths. The CS tensor components of L-glutamine and L-cystine are also included in the figure, which are consistent with the trend. As for the spectral assignment of L-histidine, the above relationship is helpful. Because the shorter C–O bond lengths exhibit the larger values of  $\delta_{22}$  components, it is safe to say that site A ( $\delta_{22} = 328 \pm 4$  ppm) and site B ( $\delta_{22} = 318 \pm 4$  ppm) are assigned to be O1 (C–O = 1.248 Å) and O2 (C–O = 1.250 Å), respectively. From the fitting equation in Fig. 9, C–O bond lengths can be estimated when the magnitudes of  $\delta_{22}$  components are experimentally derived. From the present data, the C–O bond lengths of L-asparagine are estimated to be approximately 1.235 and 1.255 Å.

*[ $^{17}\text{O}$ ]-L-Tryptophanyl-glycyl-glycine dihydrate*  
(*[ $^{17}\text{O}$ ]WGG*)

Solid-state  $^{17}\text{O}$  NMR is expected to be a useful technique for investigating biological macromolecules such as proteins and enzymes. Recently, our group has developed an efficient  $^{17}\text{O}$  labeling method for amino acids and peptides [9]. Towards future applications to proteins, we synthesized a linear tripeptide, L-tryptophanyl-glycyl-glycine dihydrate (WGG), in which the amide oxygen of the tryptophan-residue was exchanged with  $^{17}\text{O}$ , and  $^{17}\text{O}$  NMR experiments were performed. Fig. 10 shows the experimental and calculated  $^{17}\text{O}$  MAS NMR spectrum for [ $^{17}\text{O}$ ]WGG with a sample spinning frequency of  $15.00 \pm 0.06$  kHz.

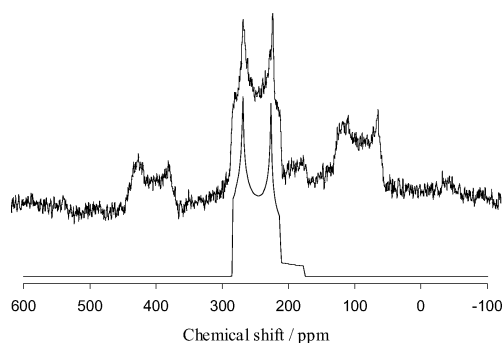


Fig. 10. Experimental and calculated 1D  $^{17}\text{O}$  MAS spectra of  $[^{17}\text{O}]$ -L-tryptophanyl-glycyl-glycine dihydrate measured at 16.4 T.

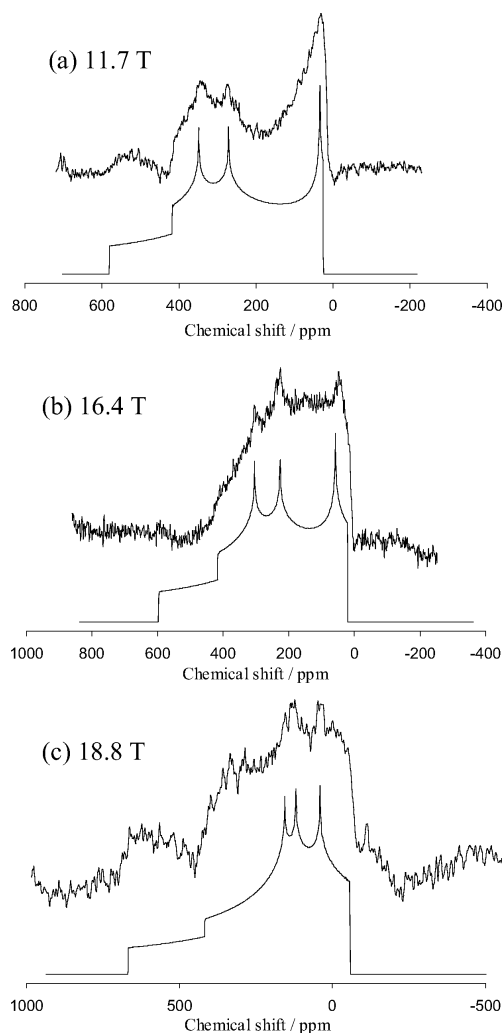


Fig. 11. Experimental and calculated  $^{17}\text{O}$  stationary spectra of  $[^{17}\text{O}]$ -L-tryptophanyl-glycyl-glycine observed at (a) 11.7, (b) 16.4, and (c) 18.8 T.

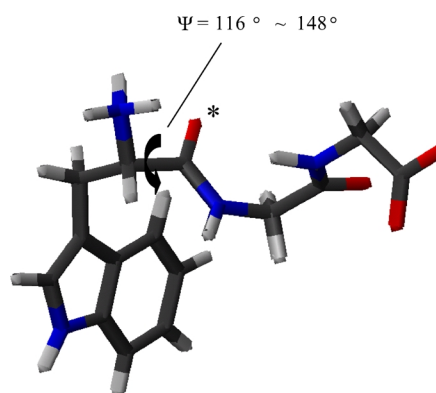


Fig. 12. Model of L-tryptophanyl-glycyl-glycine used in the quantum chemical calculations where the torsion angle,  $\psi$ , was varied from  $\psi = 116 - 148^\circ$  in steps of  $4^\circ$ . The  $^{17}\text{O}$  NMR parameters for the oxygen atom marked by \* were calculated with the B3LYP/D95\*\* level of theory.

Although a few spinning sidebands appeared on the MAS spectrum, it could be fitted to a typical line shape arising from the second-order quadrupole interaction. The analysis of the 1D MAS spectra yielded the following parameters for  $[^{17}\text{O}]$ WGG:  $\delta_{\text{iso}} = 297 \pm 4$  ppm,  $C_Q = 8.4 \pm 0.1$  MHz,  $\eta_Q = 0.24 \pm 0.04$ . Fig. 11 shows the experimental and calculated  $^{17}\text{O}$  stationary NMR spectra for  $[^{17}\text{O}]$ WGG, observed at (a) 11.7 T, (b) 16.4 T, and (c) 18.8 T. The obtained  $^{17}\text{O}$  NMR parameters are summarized in Table 1. The experimental orientation of  $^{17}\text{O}$  CS and EFG tensors with respect to the molecular frame for  $[^{17}\text{O}]$ WGG is shown in Fig. 8(b). The obtained parameters are consistent with the previous determination for primary and secondary amides, and small peptides [5, 7, 10]. As can be seen in Table 1, the magnitudes of the  $C_Q$  values and the  $\delta_{11}$  components for the peptide are larger than those for individual amino acids. It is interesting to note that, for  $^{17}\text{O}$  EFG tensors, orientations are essentially the same for the amino acids and peptides, but, for  $^{17}\text{O}$  CS tensors, they are different. This suggests that  $^{17}\text{O}$  CS tensor orientations as well as their magnitudes are also sensitive to the local chemical environments.

$\alpha$ -Helix and  $\beta$ -sheet are common components of the structures of proteins, and such secondary structures are well described by two dihedral angles,  $\phi$  and  $\psi$ . Because  $^{17}\text{O}$  NMR parameters are highly sensitive to the local chemical environments, it is expected that  $^{17}\text{O}$  NMR tensors are related with changes of dihedral angles. To investigate the dihedral angle dependence of  $^{17}\text{O}$  NMR parameters, we have constructed

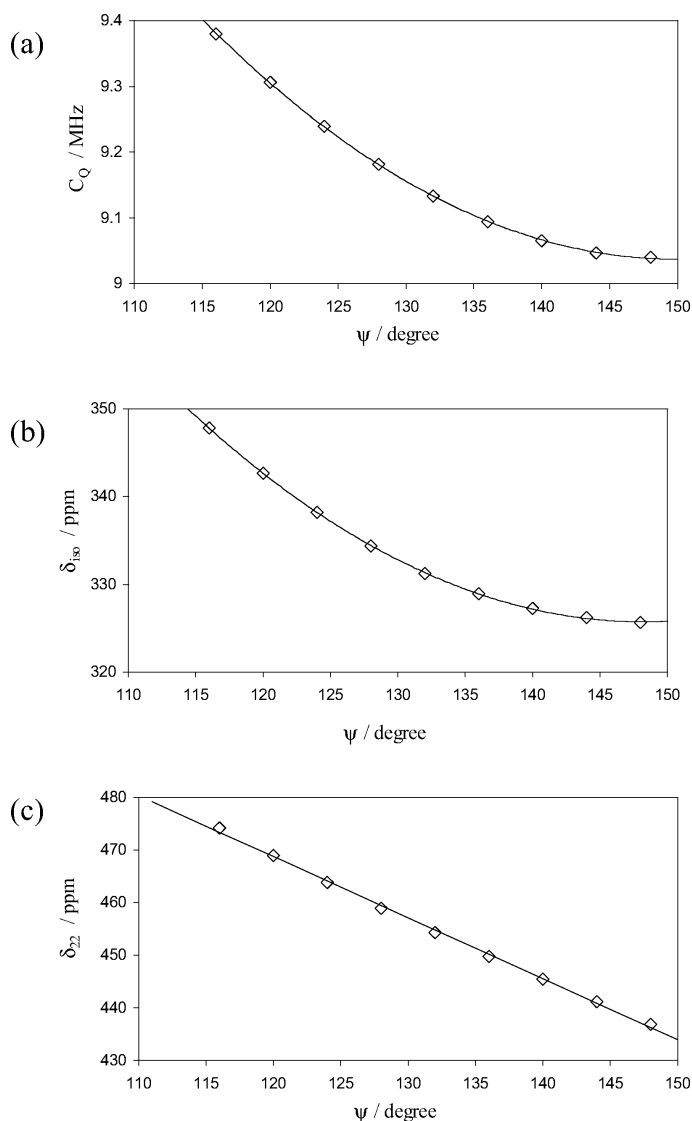


Fig. 13. Calculated  $^{17}\text{O}$  (a) quadrupole coupling constants, (b) isotropic chemical shifts, and (c)  $\delta_{22}$  components *versus* the dihedral angles for the model of L-tryptophanyl-glycyl-glycine in Fig. 12.

a simple model of an isolated tripeptide molecule, WGG, in which the torsion angle,  $\psi$ , is artificially changed from  $116^\circ$  to  $148^\circ$  in steps of  $4^\circ$ , as is shown in Fig. 12. The quantum chemical calculations for the amide oxygen in the tryptophan-residue were performed at the B3LYP/D95\*\* level of theory. The experimental geometry of the WGG [18] was originally used for these calculations. Table 3 summarizes the results of  $^{17}\text{O}$  NMR calculations for the torsion angle model. Fig. 13 indicates the dependence of the carbonyl  $^{17}\text{O}$  (a) quadrupole coupling constants and (b) isotropic chemical shifts on the torsion angles. It can be observed that, with increase in the torsion an-

gles, the values of both  $C_Q$  and  $\delta_{\text{iso}}$  gradually decrease. This indicates that the  $^{17}\text{O}$  NMR parameters are potentially sensitive to the changes of the conformation of the backbone chain in proteins. One interesting finding is that the values of  $\delta_{22}$  components are linearly correlated with the dihedral angles, as shown in Fig. 13(c). It is of interest to further investigate the relationship between the  $^{17}\text{O}$  NMR parameters and the secondary structures of peptides and proteins since  $^{17}\text{O}$  NMR may become a new nucleus probe for investigating the functions and structures of proteins in the near future. Such studies are in progress in our group.

## Experimental Section

### Sample aspects

$^{17}\text{O}$ -enriched L-glutamine, L-asparagine, L-cystine, and L-histidine were obtained by the saponification of the corresponding Fmoc-protected pentafluorophenyl esters with  $\text{H}_2^{17}\text{O}$  (80–85 atom-%, purchased from TAIYO NIPPON SANSO, Tokyo, Japan). In order to yield free amino acids, deprotection of *N*-terminal protecting groups was achieved by treatment with piperidine/dimethyl formamide (2 : 8) solutions. The protecting groups of side chains were removed using trifluoroacetic acid/ethanedithiol/thioanisole (90 : 5 : 5) solutions. The white crystalline crudes were purified by ion-exchange chromatography. Detailed procedures have been described elsewhere [9]. The solution NMR and MS results for the present compounds were in a good agreement with the literature values. The enrichment ratios of L-glutamine, L-asparagine, L-cystine, and L-histidine were 74, 74, 85, and 64 %, respectively. Powder X-ray diffraction was carried out on a Rigaku Ultima+ diffractometer using  $\text{CuK}\alpha$  radiation at a wavelength of 1.54184 Å. The diffraction patterns were recorded in the range  $2\theta = 3.00$ – $90.00^\circ$  in  $0.02^\circ$  steps with a scan rate of  $10 \text{ deg min}^{-1}$  at r. t. From the results, the space groups of L-glutamine, L-asparagine, L-cystine, and L-histidine were confirmed to be  $P2_12_12_1$  ( $Z = 4$ ,  $a = 7.766$ ,  $b = 16.027$ ,  $c = 5.103$  Å) [19],  $P2_1$  ( $Z = 2$ ,  $a = 8.074$ ,  $b = 6.768$ ,  $c = 5.070$  Å,  $\beta = 91.35^\circ$ ) [20],  $P6_122$  ( $Z = 6$ ,  $a = 5.426$ ,  $c = 56.34$  Å) [21], and  $P2_12_12_1$  ( $Z = 4$ ,  $a = 5.143$ ,  $b = 7.294$ ,  $c = 18.674$  Å) [22], respectively.  $^{17}\text{O}$ -enriched  $N_\alpha$ -Fmoc- $N_{(\text{in})}$ -Boc-L-tryptophan was obtained in a similar manner to the above. Using the  $^{17}\text{O}$ -enriched Fmoc-protected amino acid, L-tryptophanyl-glycyl-glycine dihydrate was synthesized on the basis of standard solid-phase peptide synthesis protocols. The solution NMR and MS results were in a good agreement with the literature values.

### Solid-state $^{17}\text{O}$ NMR

All the  $^{17}\text{O}$  NMR experiments were performed on a Chemagnetics Infinity-400 spectrometer, JEOL ECA 500 and 700 spectrometers, and a Bruker Avance-800 spectrometer operating at frequencies of 54.21, 67.87, 94.98, and 108.5 MHz, respectively. Polycrystalline amino acids were packed into 4-mm rotors of either zirconium oxide or silicon nitride. An external sample of liquid water was employed for chemical shift referencing. The recycle delay was typically 5–10 s.  $^{17}\text{O}$  3QMCMAS experiments were carried out on the JEOL ECA 700 spectrometer. The z-filter pulse sequence proposed by Amoureux *et al.* [23] was employed. A home-built probe was used and the radio frequency field strengths for MQ excitations and conversion pulses at 94.98 MHz were approximately 200–250 kHz. All the NMR spectra were processed by either MestReC 2.3a [24], or Delta (JEOL USA, Inc.) software. Spectral

simulations were performed on a Pentium IV personal computer (3.00 GHz, 1 GB memory, 200 GB disk space) using the program written by the authors on MATLAB (The MathWorks, Inc.).

### Quantum chemical calculations

All quantum chemical calculations on  $^{17}\text{O}$  EFG and CS tensors were performed with the Gaussian03 program package [25] on the RIKEN Super Combined Cluster (RSCC). The crystal structures of the amino acids and the tripeptide were derived from the Cambridge Structural Database [26].

The Gauge-Induced Atomic Orbital (GIAO) approach [27, 28] was used for chemical shielding calculations. In NMR experiments, the frequency of an NMR signal is observed relative to that in a reference system. For  $^{17}\text{O}$  NMR, liquid water is generally used as the reference. Because the quantum calculations give absolute chemical shielding values,  $\sigma_{\text{ii}}$ , it is convenient to convert them into chemical shifts relative to water,  $\delta_{\text{ii}}$ , by using

$$\delta_{\text{ii}} = 307.9 - \sigma_{\text{ii}} \text{ [ppm]} \quad (1)$$

where the value of 307.9 ppm is the absolute chemical shielding constant for the  $^{17}\text{O}$  nucleus in liquid  $\text{H}_2\text{O}$  [29].

The quantum chemical calculations yield EFG tensors in atomic units (a. u.),  $q_{\text{ii}}$ . In solid-state NMR experiments, quadrupolar coupling interactions are expressed as EFG tensors in frequency whose principal components are defined as  $|V_{\text{xx}}| < |V_{\text{yy}}| < |V_{\text{zz}}|$ . To describe a traceless EFG tensor, one uses two NMR parameters, namely, the quadrupole coupling constant,  $C_Q$ , and the asymmetry parameter,  $\eta_Q$ . The following equations were employed for making a direct comparison between theoretical and experimental data:

$$C_Q \text{ [MHz]} = eV_{\text{zz}}Qh^{-1} = -2.3496Q \text{ [fm}^2\text{]}q_{\text{zz}} \text{ [a. u.]} \quad (2)$$

and

$$\eta_Q = (V_{\text{xx}} - V_{\text{yy}})/V_{\text{zz}} \quad (3)$$

where  $Q$  is the electric quadrupole moment of the  $^{17}\text{O}$  nucleus and the factor of 2.3496 comes from unit conversion. In the present calculations,  $Q = -2.558 \text{ fm}^2$  [30] was employed in all EFG calculations.

### Acknowledgments

This research was financially supported by the Ministry of Education, Science, Sports, Culture, and Technology (MEXT) of Japan for National Project on Protein Structural and Functional Analyses, *Protein 3000*. K. Y. thanks MEXT for funding the work on solid-state  $^{17}\text{O}$  NMR of peptides and proteins (Young Scientists (B), 17750171). We thank Dr. Daisuke Hashizume for his help with the powder X-ray diffraction experiments. We wish to thank Ikuko Maeda and

Dr. Hiroshi Ono for their assistance in NMR experiments at the National Food Research Institute. We also wish to thank Shinobu Ohki, Kenzo Deguchi, and Teruaki Fujito for their

technical assistance at the National Institute for Materials Science. Finally, we are grateful to an anonymous reviewer for helpful comments.

- [1] L. Frydman, J. S. Harwood, *J. Am. Chem. Soc.* **1995**, *117*, 5367.
- [2] A. Medek, J. S. Harwood, L. Frydman, *J. Am. Chem. Soc.* **1995**, *117*, 12779.
- [3] V. Lemaitre, K. J. Pike, A. Watts, T. A. Anupold, A. Samoson, M. E. Smith, R. Dupree, *Chem. Phys. Lett.* **2003**, *371*, 91.
- [4] K. J. Pike, V. Lemaitre, A. Kukol, T. Anupold, A. Samoson, A. P. Howes, A. Watts, M. E. Smith, R. Dupree, *J. Phys. Chem. B* **2004**, *108*, 9256.
- [5] V. Lemaitre, M. R. R. De Planque, A. P. Howes, M. E. Smith, R. Dupree, A. Watts, *J. Am. Chem. Soc.* **2004**, *126*, 15320.
- [6] C. Gervais, R. Dupree, K. J. Pike, C. Bonhomme, M. Profeta, C. J. Pickard, F. Mauri, *J. Phys. Chem. A* **2005**, *109*, 6960.
- [7] J. Hu, E. Y. Chekmenev, Z. Gan, P. L. Gor'kov, S. Saha, W. W. Brey, T. A. Cross, *J. Am. Chem. Soc.* **2005**, *127*, 11922.
- [8] A. Steinschneider, M. I. Burgar, A. Buku, D. Fiat, *Int. J. Peptide Protein Res.* **1981**, *18*, 324.
- [9] K. Yamada, T. Yamazaki, M. Asanuma, H. Hirota, N. Yamamoto, Y. Kajihara, *Chem. Lett.* **2007**, *36*, 192.
- [10] K. Yamada, S. Dong, G. Wu, *J. Am. Chem. Soc.* **2000**, *122*, 11602.
- [11] K. Yamada, H. Honda, T. Yamazaki, M. Yoshida, *Solid State Nucl. Magn. Reson.* **2006**, *30*, 262.
- [12] K. Yamada, M. Asanuma, H. Honda, T. Nemoto, T. Yamazaki, H. Hirota, *J. Mol. Struct.*, in press.
- [13] T. F. Koetzle, M. N. Frey, M. S. Lehmann, W. C. Hamilton, *Acta Cryst.* **1973**, *B29*, 2571.
- [14] B. M. Oughton, P. M. Harrison, *Acta Cryst.* **1959**, *12*, 396.
- [15] J. J. Madden, E. L. McGandy, N. C. Seeman, *Acta Cryst.* **1972**, *B28*, 2377.
- [16] J. R. Yates, C. J. Pickard, M. C. Payne, R. Dupree, M. Profeta, F. Mauri, *J. Phys. Chem. A* **2004**, *108*, 6032.
- [17] K. Yamada, T. Shimizu, M. Tansho, T. Nemoto, M. Asanuma, M. Yoshida, T. Yamazaki, H. Hirota, *Magn. Reson. Chem.*, in press.
- [18] E. Subramanian, J. Sahayamary, *Int. J. Peptide Protein Res.* **1989**, *34*, 134.
- [19] International Centre for Diffraction Data, Powder Diffraction Data, Card 39-1835.
- [20] International Centre for Diffraction Data, Powder Diffraction Data, Card 37-1659.
- [21] International Centre for Diffraction Data, Powder Diffraction Data, Card 37-1802.
- [22] International Centre for Diffraction Data, Powder Diffraction Data, Card 51-2290.
- [23] J. P. Amoureux, C. Fernandez, S. Steuernagel, *J. Magn. Reson.* **1996**, *123*, 116.
- [24] J. C. Cobas, F. J. Sardina, *Concepts Magn. Reson.* **2003**, *19A*, 80.
- [25] M. J. Frisch, G. W. Trucks, H. B. Schlegel, G. E. Scuseria, M. A. Robb, J. R. Cheeseman, J. A. Montgomery, Jr., T. Vreven, K. N. Kudin, J. C. Burant, J. M. Millam, S. S. Iyengar, J. Tomasi, V. Barone, B. Menucci, M. Cossi, G. Scalmani, N. Rega, G. A. Petersson, H. Nakatsuji, M. Hada, M. Ehara, K. Toyota, R. Fukuda, J. Hasegawa, M. Ishida, T. Nakajima, Y. Honda, O. Kitao, H. Nakai, M. Klene, X. Li, J. E. Knox, H. P. Hratchian, J. B. Cross, V. Bakken, C. Adamo, J. Jaramillo, R. Gomperts, R. E. Stratmann, O. Yazyev, A. J. Austin, R. Cammi, C. Pomelli, J. W. Ochterski, P. Y. Ayala, K. Morokuma, G. A. Voth, P. Salvador, J. J. Dannenberg, V. G. Zakrzewski, S. Dapprich, A. D. Daniels, M. C. Strain, O. Farkas, D. K. Malick, A. D. Rabuck, K. Raghavachari, J. B. Foresman, J. V. Ortiz, Q. Cui, A. G. Baboul, S. Clifford, J. Cioslowski, B. B. Stefanov, G. Liu, A. Liashenko, P. Piskorz, I. Komaromi, R. L. Martin, D. J. Fox, T. Keith, M. A. Al-Laham, C. Y. Peng, A. Nanayakkara, M. Challacombe, P. M. W. Gill, B. Johnson, W. Chen, M. W. Wong, C. Gonzalez, J. A. Pople, GAUSSIAN 03 (Revision B.05), Gaussian, Inc., Wallingford CT (USA) **2004**.
- [26] D. Fletcher, R. McMeeking, D. Parkin, *J. Chem. Inf. Comput. Sci.* **1996**, *36*, 746.
- [27] R. Ditchfield, *Mol. Phys.* **1974**, *27*, 789.
- [28] K. Wolinski, J. F. Hilton, P. Pulay, *J. Am. Chem. Soc.* **1990**, *112*, 8257.
- [29] R. E. Wasylshen, S. Mooibroek, J. B. Macdonald, *J. Chem. Phys.* **1984**, *81*, 1057.
- [30] P. Pyykkö, *Z. Naturforsch.* **1992**, *47a*, 189.